



OPEN ACCESS

EDITED BY
Kit Lai,
Fortescue Metals Group, Australia

REVIEWED BY
Junming Yao,
Xinjiang Institute of Ecology and
Geography (CAS), China
Changzhou Deng,
Institute of Geochemistry (CAS), China

*CORRESPONDENCE
Guangzhou Mao,
✉ gzmaonjunwu@163.com
Mingping Cao,
✉ cmp4688164@163.com

SPECIALTY SECTION
This article was submitted to
Economic Geology,
a section of the journal
Frontiers in Earth Science

RECEIVED 31 October 2022
ACCEPTED 28 December 2022
PUBLISHED 12 January 2023

CITATION
Li Z, Mao G, Liu C, Liu X, An P and Cao M
(2023), Nature and geochemical
characteristics of ore-forming fluids in the
Zhaoxian gold deposit, Jiaodong gold
province, eastern China.
Front. Earth Sci. 10:1085398.
doi: 10.3389/feart.2022.1085398

COPYRIGHT
© 2023 Li, Mao, Liu, Liu, An and Cao. This is
an open-access article distributed under
the terms of the [Creative Commons
Attribution License \(CC BY\)](https://creativecommons.org/licenses/by/4.0/). The use,
distribution or reproduction in other
forums is permitted, provided the original
author(s) and the copyright owner(s) are
credited and that the original publication in
this journal is cited, in accordance with
accepted academic practice. No use,
distribution or reproduction is permitted
which does not comply with these terms.

Nature and geochemical characteristics of ore-forming fluids in the Zhaoxian gold deposit, Jiaodong gold province, eastern China

Zhi Li^{1,2,3}, Guangzhou Mao^{1,2,3*}, Caijie Liu^{3,4}, Xiaotong Liu^{1,5}, Pengrui An¹ and Mingping Cao^{1*}

¹Shandong Provincial Key Laboratory of Depositional Mineralization & Sedimentary Minerals, College of Earth Sciences & Engineering, Shandong University of Science and Technology, Qingdao, Shandong, China, ²Functional Laboratory of Marine Mineral Resources Evaluation and Detection Technology, Qingdao National Laboratory of Marine Science and Technology, Qingdao, Shandong, China, ³Shandong Provincial Engineering Laboratory of Application and Development of Big Data for Deep Gold Exploration, Weihai, Shandong, China, ⁴No. 6 Institute of Geology and Mineral Resources Exploration, of Shandong Province, Shandong, China, ⁵Agency for Natural Resources of Rongcheng, Weihai, Shandong, China

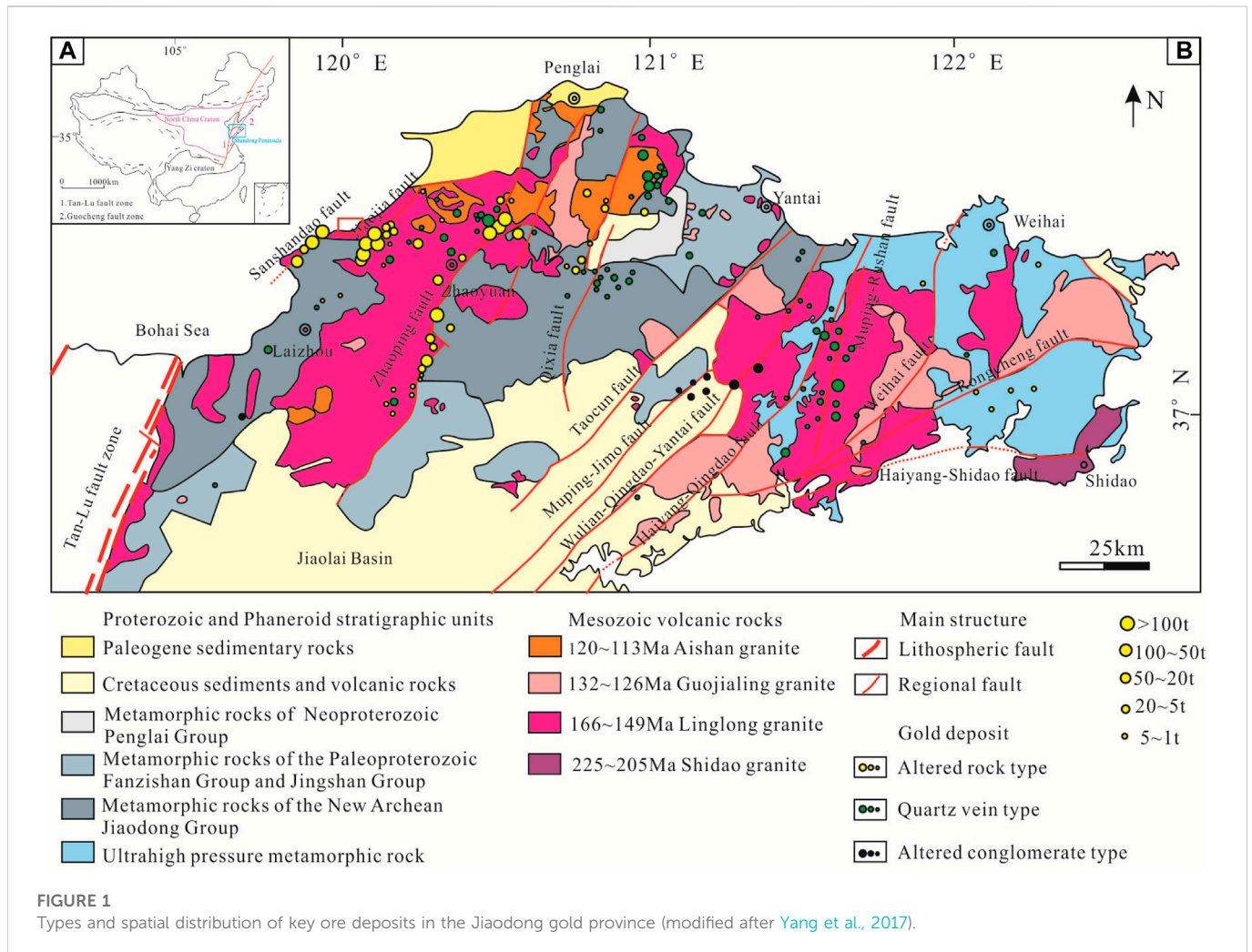
KEYWORDS

fluid inclusions, trace elements, ore genesis, Zhaoxian gold deposit, Jiaodong gold province

Introduction

Jiaodong is the most prolific gold province in China. Based on the spatial distribution and structural characteristics of gold deposits, the province can be divided into three ore belts, i.e., (from west to east) the Laizhou-Zhaoyuan-Pingdu, Penglai-Qixia, and Muping-Rushan (Chen et al., 1989). The Jiaodong gold deposits are usually divided into three types: altered-rock type (aka. Jiaojia type, e.g., Jiaojia, Sanshandao, Xiadian, and Xincheng) (Li, 1988; Lu et al., 1999a; Wen et al., 2016; Ma et al., 2017), quartz vein type (aka. Linglong type, e.g., Linglong, Jiuqu, and Baotouqing) (Qiu et al., 1988; Lu et al., 1999b; Yang et al., 2016a) and pyrite-carbonate type (aka. Liaoshang type, incl. Liaoshang, Tudui, and Shawang) (Li et al., 2017). Many previous studies have analyzed the source and properties of ore-forming fluids of the Jiaodong gold deposits, with the main findings include: 1) the ore-forming fluids have had input from the mantle (Deng et al., 2015; Liang et al., 2015), magmatic water (Zhao et al., 2015; Zhang et al., 2017), and a mixture of metamorphic-hydrothermal fluids and meteoric water (Xu et al., 2016; Tan et al., 2018); 2) the ore-forming fluids likely changed from early-stage medium-high temperature and medium-low salinity to late-stage medium-low temperature and low salinity (Wang et al., 2014; Yan et al., 2014; Deng et al., 2015; Yang et al., 2017); 3) the ore-forming materials may have sourced from the mantle, Yanshanian (Jurassic-Cretaceous) granites, and Yanshanian (Jurassic-Cretaceous) granite-greenstone (Zhou et al., 2000; Zhang et al., 2014; Deng et al., 2015; Yang et al., 2016b). However, some workers argued that ore-forming fluids of the different ore types are not very different, and the physicochemical properties and interpreted ore-fluid sources are largely the same. This implies that these different types of gold deposits were formed in the same ore-forming event, and the ore geological differences were likely caused by the ore-controlling structures (Yang et al., 2006).

The Zhaoxian gold deposit (altered-rock type) is located at the junction between the Sanshandao-Cangshang and Laizhou-Longkou gold belts. Built on previous works, our study focuses on the trace element compositions (e.g., Rb, Ta, Nb, Sr, Zr, Hf) of fluid inclusions and ore-stage granite at Zhaoxian. We discuss the ore-fluid properties, the ore-material source(s), and the gold metallogeny at Zhaoxian, in order to provide reference for regional gold exploration and research.



Regional geology

The Jiaodong gold province is located in the eastern part of Tanlu fault zone, which is the tectonic junction of the North China Craton, Yangtze Block and Qinling-Dabie Orogen (Figure 1A). The province comprises (from north the south) the Jiaobei uplift, Jiaolai basin, and Sulu ultra-high pressure (UHP) belt (Figure 1B) (Li et al., 2007; Tan et al., 2012; Li, 2016). Rocks in the province include mainly Precambrian metamorphic basement rocks and Mesozoic magmatic rocks. The former includes the Archean Jiaodong Group (incl. Neoproterozoic Qixia tonalite-diorite gneiss and Malianzhuang metagabbro), Paleoproterozoic Jingshan and Fanzishan Groups, and the Neoproterozoic Penglai Group (Tang et al., 2007; Tang et al., 2008; Zhai and Santosh., 2013); The Mesozoic magmatic rocks include mainly ca. 160–150 Ma crustal source Linglong medium-grained biotite monzogranite, ca. 130–126 Ma Guojialing granodiorite with a crust-mantle mixed origin (Yang et al., 2012; Yang et al., 2014), and the intermediate-mafic dikes (incl. lamprophyre, diorite porphyrite, and diabase porphyrite). Gold deposits are mainly hosted in the Linglong granite and Guojialing granodiorite, and the contact zone between the granite and Precambrian metamorphic rocks. Tectonic activity in the northwestern Jiaodong region has formed brittle and brittle structures (Li et al., 2003; Song et al., 2020). The Sanshandao,

Jiaojia, and Zhaoping faults are the main ore-controlling structures in the region, which control the formation and distribution of gold deposits (Song et al., 2010a).

Deposit geology

Stratigraphy, structure, and magmatic-metamorphic rocks

At the Zhaoxian gold deposit, exposed pre-Quaternary strata comprise mainly the Paleoproterozoic Lugezhuang Formation (Jingshan Group) granulite, marble and schist, and the Cenozoic Zhubidian Formation (Wutu Group) pebbly feldspar sandstone and clayey sandstone (Zhu, 2018). The Jiaojia fault (~60 km long, max 1 km wide) at Zhaoxian is divided into three segments, i.e., (from north to south) the Gaojiashuangzi-Xincheng, Xincheng-Jiaojia (Matang), and Sizhuang. The fault strikes 30°–50° and has a dip angle of 80° (Shu et al., 2022). The Jiaojia fault branches out into secondary structures locally and is featured by multistage movements (Song et al., 2010b; Hen et al., 2015; Cao et al., 2016; Sun et al., 2018). Magmatic rocks are widely distributed at Zhaoxian, and comprise (from old to young) the meta-gabbro in the Neoproterozoic Malianzhuang sequence (Figure 2), the Qixia

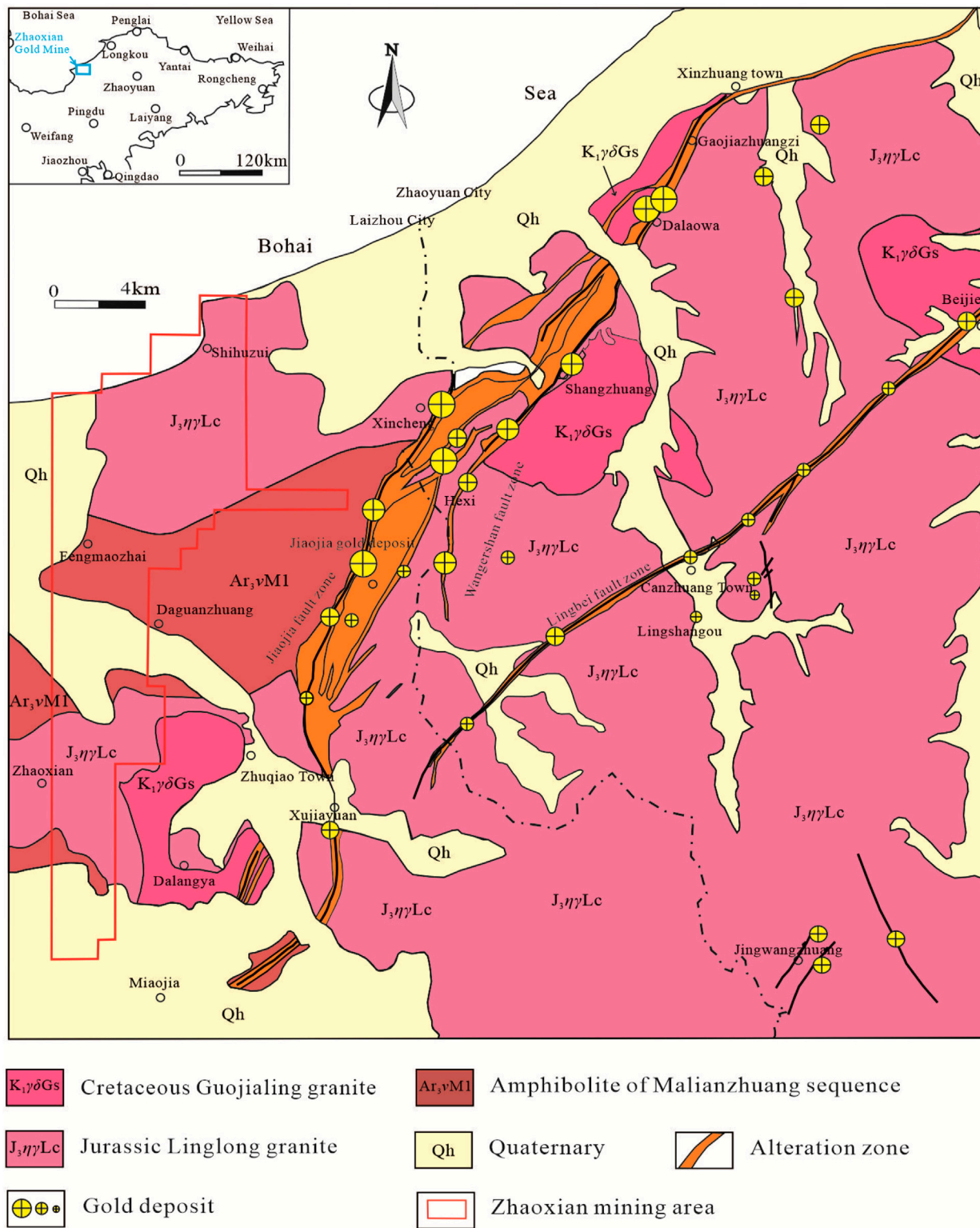
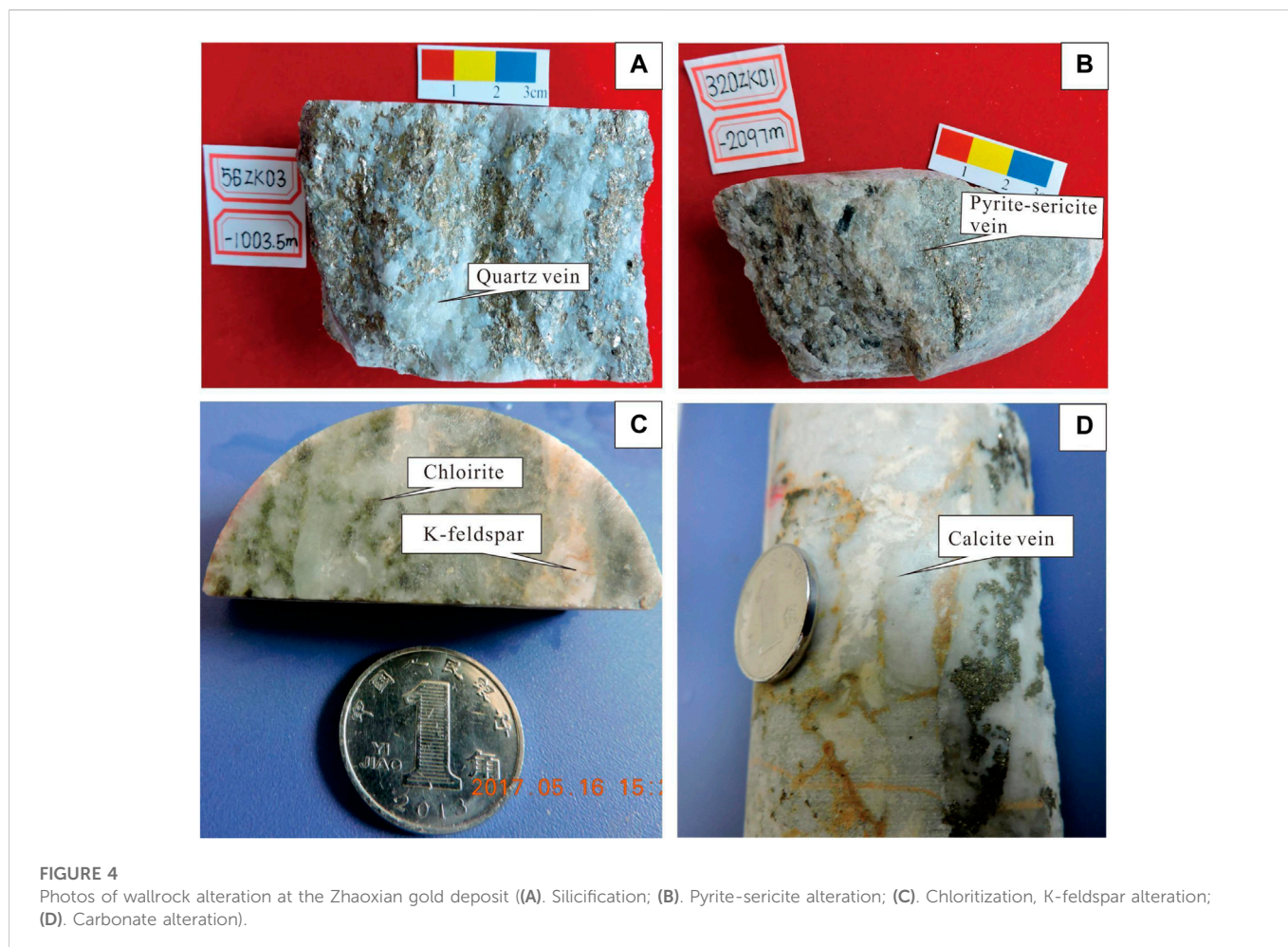
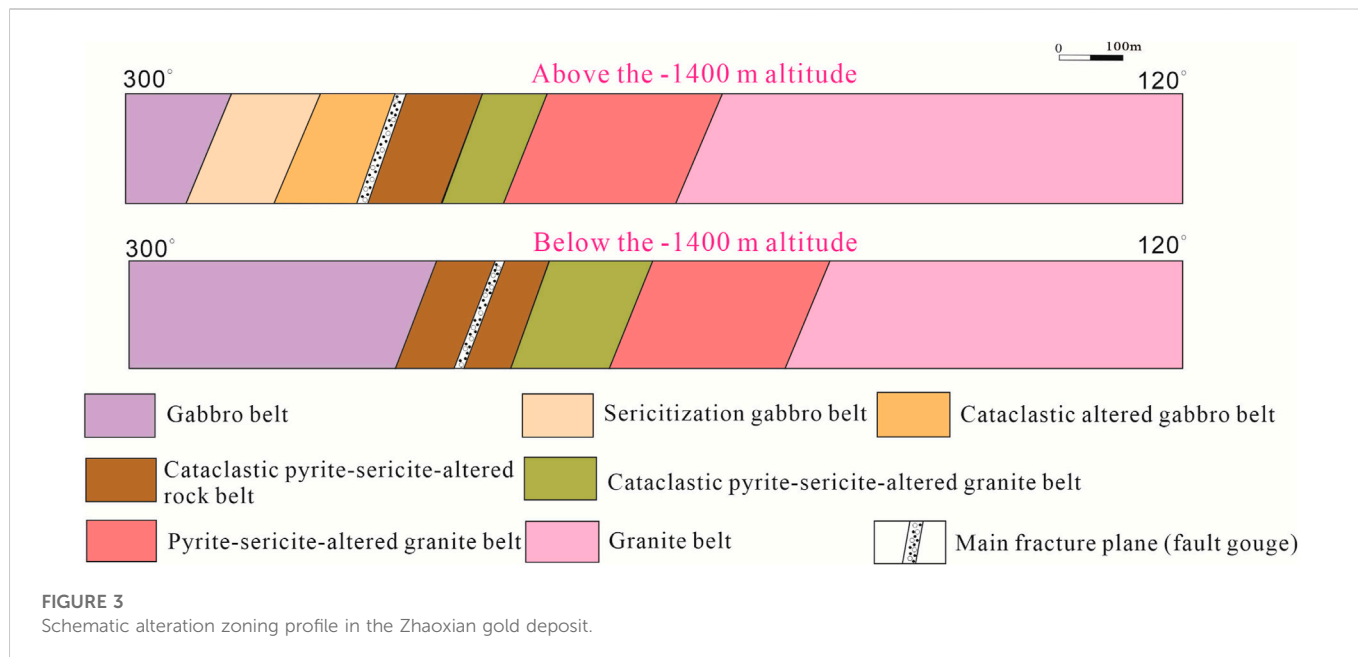


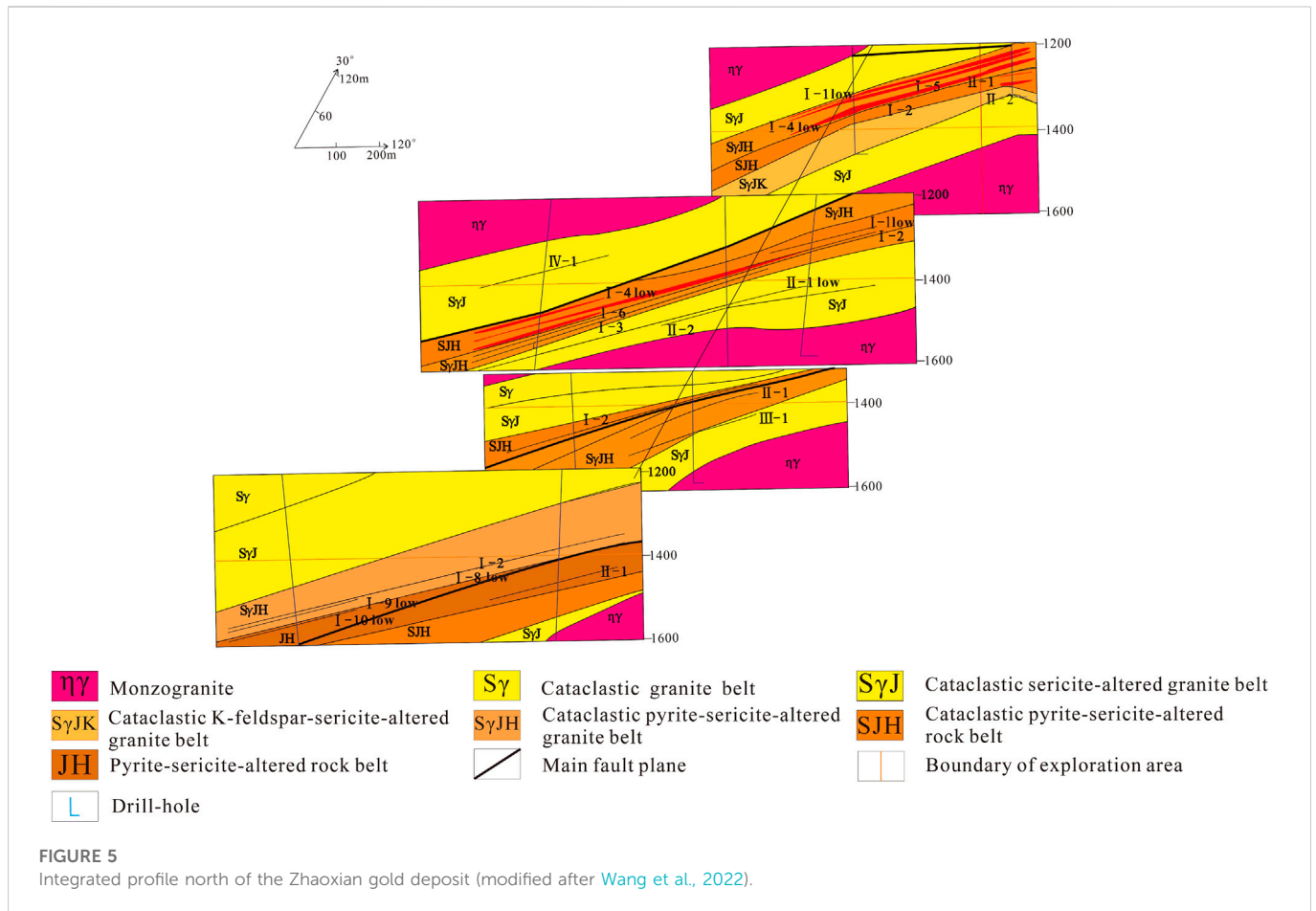
FIGURE 2 Geological and mineral map of the study area (modified after Song et al., 2018).

gneiss, biotite tonalite, (weakly gneissic) early Yanshanian Linglong medium-grained monzogranite, the late Yanshanian Guojialing porphyritic granodiorite, and some younger dykes (Song et al., 2010b).

Wallrock alteration

Alteration is well developed along the faults at Zhaoxian. In the hanging-wall, there is a cataclastic zone with sericitized wallrocks,





which transitions into a partially pyrite-sericite-altered cataclastic zone. The footwall also contains a pyrite-sericite-altered cataclastic zone, which transitions into pyrite-sericite alteration in the granite wallrocks (Figure 3).

Major alteration styles in the wallrocks include mainly 1) silicification (Figure 4A), which is often associated with metal sulfides and gold mineralization; 2) pyrite-sericite alteration (Figure 4B), with the mineral assemblage of sericite + quartz ± pyrite in cataclastic rocks; 3) chloritization (Figure 4C), which is altered from magmatic hornblende and biotite, occurring locally as patches or veinlets; 4) K-feldspar alteration (Figure 4C), which occurred in an early hydrothermal stage and the altered rocks have a fleshy red color; 5) carbonate alteration (Figure 4D), which occurs as late calcite veining (cutting the ores) and locally massive aggregates.

Orebody characteristics

The orebodies at Zhaoxian can be divided into four groups (I to IV) (Figure 5): I) The orebodies in the pyrite-sericite-altered cataclastic zone on the footwall (Figure 5), containing 20 orebodies and accounting for 71.04% of the estimated total resource. Among them, No. I-2 orebody is the main orebody, accounting for 42.44% of the total resource; II) The orebodies in the pyrite-sericite-altered granitic cataclastic zone below Group I (Figure 5), containing 13 orebodies and accounting for 19.93% of the estimated total resource. Among them, No. II-1 orebody is one of the largest,

accounting for 10.48% of the total resource; III) The nine orebodies in the pyrite-sericite-altered granite belt below Group II (Figure 5), accounting for 3.95% of the estimated total resource; IV) The orebodies in the pyrite-sericite-altered granite cataclastic zone above the main fault surface (Figure 5), containing seven orebodies and accounting for 5.08% of the estimated total resource.

Alteration and mineralization paragenesis

Based on the field crosscutting relationships and mineral assemblages, the alteration/mineralization at Zhaoxian can be divided into four stages, namely (from old to young):

- 1) Pyrite-quartz-K-feldspar (Figures 6A,B): Pyrite is coarse-grained subhedral, and occurs as patches and veins with cataclastic texture. The quartz is coarse-grained milky and with wavy extinction. The K-feldspar is coarse-grained anhedral granular, and is commonly altered to sericite in the later hydrothermal stages. At this stage, minor native gold mineralization is observed under the microscope. The gold particles are small and mostly included in pyrite.
- 2) Pyrite-quartz-sericite ± chlorite (Figures 6C,D): The pyrite is fine-grained (mostly 50–300 μm) euhedral with local corroded margin. The quartz and sericite were derived from the alteration of stage I minerals. Stage 2 gold occurs mainly in inclusions or fissures.
- 3) Polymetallic sulfide-quartz (Figures 6E–G): This stage is featured by fine-grained quartz + sulfides (galena, pyrite, chalcopyrite,

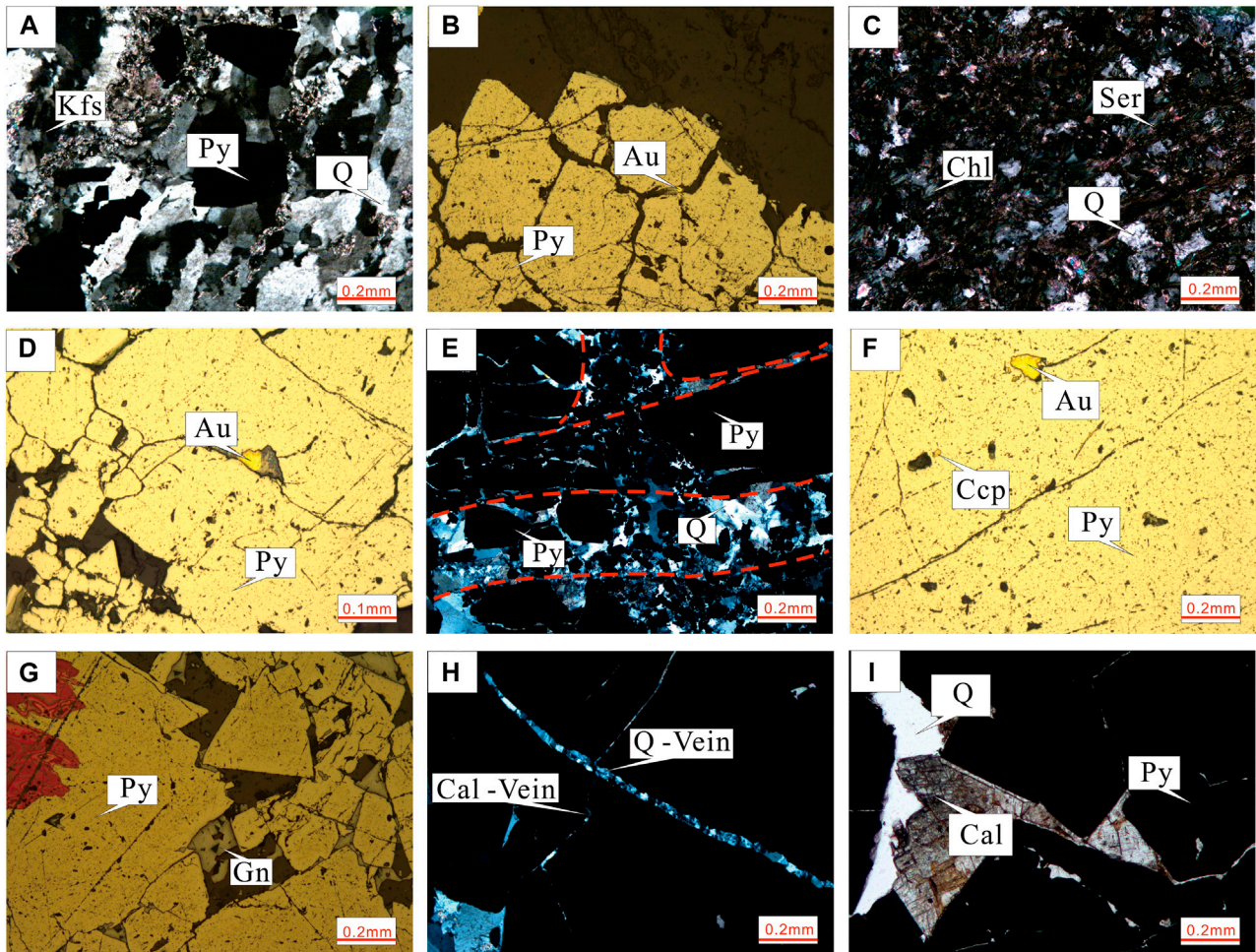


FIGURE 6

Photomicrographs of ores and altered rocks from the different metallogenic stages at Zhaoxian: (A) and (B) Pyrite-quartz-K-feldspar stage; (C) and (D) Pyrite-quartz-sericite stage; (E,F) and (G) Polymetallic sulfide-quartz stage; (H) and (I) Quartz-calcite stage. Abbreviations: Au-Native gold; Py-Pyrite; Ccp-Chalcopyrite; Gn-Galena; Q-Quartz; Kfs-K-feldspar; Chl-Chlorite; Cal-Calcite; Ser-Sericite.

sphalerite) in veinlets or disseminations, with the veinlets cutting early-stage pyrite veins. The quartz veins are smoky gray, and gold is abundant and exists in various forms, including fissure or interstitial among galena, chalcopyrite, and pyrite grains.

- 4) Quartz-calcite \pm pyrite (Figures 6H,I): Pyrite is coarse-grained (10 mm) cubic, and occurs in veins. Quartz and calcite are mainly distributed in ore-cutting veins/veinlets.

Fluid inclusion types and compositions

Sampling and analytical methods

The samples were collected from the ZK01 drill-hole at 2038–2,146 m depths (Figure 2). Because the Jiaojia fault has undergone multistage faulting and hydrothermal alteration and mineralization, we collected four ore samples at different depths to recover quartz grains from the different ore-stages. The samples consist of pyrite-sericite-altered cataclastic granite (ZX5, ZX6) and pyrite-sericite-altered clastic rock (ZX11, ZX21). The samples were prepared into double-polished thin-sections (0.3 mm thick) for optical microscopic observations. Representative

quartz-hosted fluid inclusions (FIs) from the early-ore I, main-ore (II, III), and late-ore IV) stages were selected for microthermometric and laser Raman spectroscopic analyses.

The FI microthermometric measurement was performed at the Fluid Inclusion Laboratory of the Analysis, Test and Research Center (Beijing Institute of Geology of Nuclear Industry), on a Linkam-THMS600 temperature control stage. The heating and freezing stages were calibrated by using the synthetic FI standard provided by Fluid Inc. (United States). The instrument measurement accuracy is $\pm 0.5^\circ\text{C}$ down to -120°C , $\pm 0.2^\circ\text{C}$ at -70°C – 100°C , and $\pm 2^\circ\text{C}$ at 100°C – 500°C . The heating rate is $0.2^\circ\text{C}/10^\circ\text{C}/\text{min}$, and that for the CO_2 -bearing FIs decreased to $0.2^\circ\text{C}/\text{min}$ near the melting point, and to 0.2°C – $0.5^\circ\text{C}/\text{min}$ near the freezing point and homogenization for the aqueous FIs (Hu et al., 2021). All the raw data were processed with the MacFlincor program (Brown and Hagemann, 1995). Laser Raman probe analysis (RAM) was performed at the same laboratory, using a LABHR-VIS LabRAM HR800 microlaser Raman spectrometer. The analysis used a YAG crystal frequency-doubled solid-state laser with 532 nm wavelength, 100 – $4,200\text{ cm}^{-1}$ scanning range, and 2 cm^{-1} spectral resolution. Detailed sample preparation and

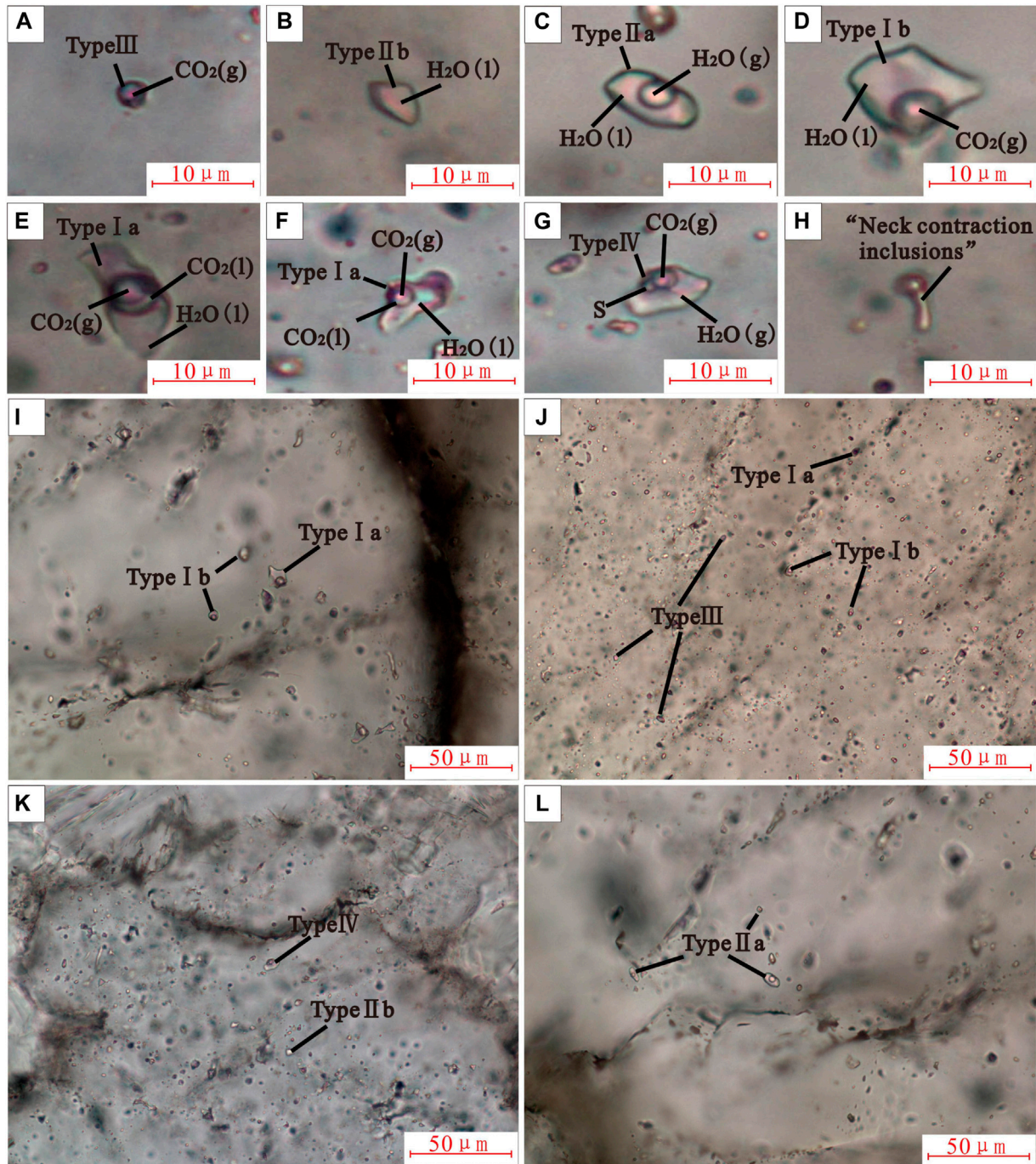


FIGURE 7 Photomicrographs of ore-stage fluid inclusions from the Zhaoxian gold deposit: (A) CO₂ single-phase; (B) aqueous single-phase; (C) two-phase aqueous inclusions; (D) two-phase H₂O + CO₂ inclusions; (E) and (F) three-phase (L_{H2O} + L_{CO2} + V_{CO2}) inclusions; (G) gaseous CO₂ and H₂O with daughter minerals; (H) neck contraction inclusions; (I) pre-ore-stage inclusions; (J) and (K) syn-ore-stage inclusions; (L) post-ore-stage inclusions.

analytical procedures follow those by [Wei et al. \(2015\)](#) and [Shu et al. \(2022\)](#).

Fluid inclusion types

Syn-ore FIs at Zhaoxian can be divided into primary and secondary ones, with the former comprising four types: CO₂-H₂O

three-phase I), H₂O aqueous II), CO₂ single-phase III) and gaseous CO₂ and H₂O with daughter minerals IV).

Type I FIs account for ~30% of the total FIs, and can be divided into two subtypes (Ia and Ib): type Ia FIs contain a liquid water phase (L_{H2O}), a liquid CO₂ phase (L_{CO2}), and a gaseous CO₂ phase (V_{CO2}) ([Figures 7E, F, I–J](#)). The L_{CO2}+V_{CO2} phase accounts for ca. 15–40 vol% of the FIs. V_{CO2} has relatively large volume. L_{CO2} usually forms a thin dark rim around V_{CO2}, and this FI type is mostly stripy. These FIs are generally 2 × 2 to 12 ×

TABLE 1 Microthermometry results of ore-stage fluid inclusions from the Zhaoxian gold deposit.

Ore stage	FI type	$Th_{rCO_2}/^{\circ}C$	$Th_{ice}/^{\circ}C$	$Th_{tot}/^{\circ}C$	Salinity (wt% NaCleqv)	Pressure (MPa)	Density (g/cm^3)
Early	Ia	28.5–31.2		234–357	3.52–11.61	261–353	0.73–0.94
	Ib, IIa		-5.4–5.6	234–276	8.03–8.41		0.83–0.97
Main	Ia	24–31.2		229–299	0.43–11.61	217–321	0.73–0.94
	Ib, IIa		-7.3–6.6	176–213	3.39–10.86		0.83–0.97
Late	Ib		-5.6–6.8	175–264	1.57–8.68		0.80–0.95

Th_{rCO_2} = partial homogenization temperature of CO_2 ; Th_{ice} = ice-freezing temperature; Th_{tot} = total homogenization temperature. The pressure is calculated with the FLINCOR, computer program, using the Th_{tot} and Th_{rCO_2} of H_2O-CO_2 three-phase inclusions (Touret, 1979; Sterner, 1991).

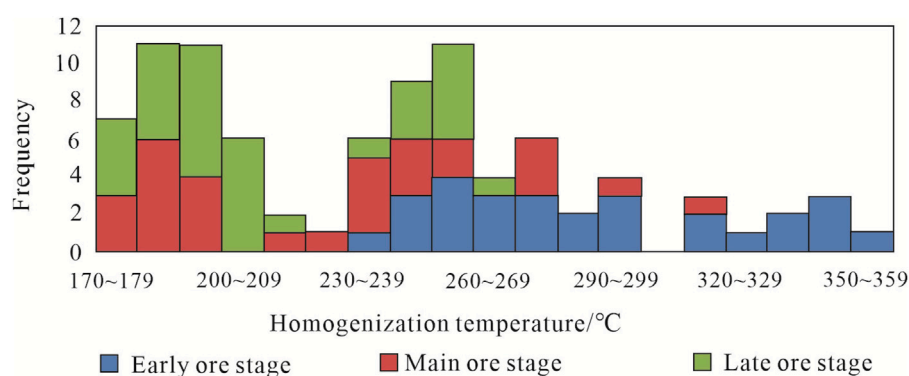


FIGURE 8

Homogenization temperature histogram of fluid inclusions from the different metallogenic stages at Zhaoxian.

14 μm in size. In type Ib two-phase ($L_{H_2O}+V_{CO_2}$) FIs (Figures 7D, I–J), the volume percentage of V_{CO_2} is largely similar (ca. 15–20 vol%). Most of these FIs are oval or negative crystal shape, with sizes of 2×3 to $4 \times 10 \mu m$ (mostly $3 \times 4 \mu m$).

Type II FIs can also be divided into two subtypes: type IIa gas-liquid ($L_{H_2O}+V_{H_2O}$) FIs (Figures 7C, L) have their gas phase accounting for ca. 15–20 vol% (and ~60% of the total number of type II FIs). They have mostly oval or negative crystal shape, with sizes of 2×3 to $4 \times 6 \mu m$ (mostly $2 \times 3 \mu m$). Type IIb (aqueous single-phase L_{H_2O}) FIs (Figures 7C, K) are colorless, transparent, and without air bubbles. They are usually long or oval shaped and are typically $2 \times 5 \mu m$ in size.

Type III FIs (Figures 7A, J) are composed of a pure CO_2 gas phase, accounting for ~7% of the total number of FIs. These inclusions are usually dark black with size of $3 \times 3 \mu m$.

Type IV FIs (Figures 7G, K) are composed of the gas phase ($V_{H_2O}+V_{CO_2}$) and daughter minerals S), and account for ~3% of the total number of FIs. Daughter minerals (size: 1–2 μm) consist mainly of halite, and occur in aqueous L_{H_2O} at room temperature. Type IV FIs are generally 4×10 to $5 \times 12 \mu m$ in size (Figures 7H).

Fluid inclusion morphology and microthermometry

Homogenization temperature and salinity

The types, distribution characteristics and microthermometric results of the primary FIs from Zhaoxian are shown in Table 1 and Figures 8 and Figure 9. Stage I quartz contains mainly type Ia ($L_{H_2O} + L_{CO_2} + V_{CO_2}$)

(Figure 7I) and type Ib ($L_{H_2O} + V_{CO_2}$) FIs (Figure 7I). Type IIa ($L_{H_2O} + V_{H_2O}$) FIs are also uniformly distributed, commonly with small size ($2 \times 3 \mu m$). Type Ia FIs are homogenized partially to gaseous or liquid phase at $28.5^{\circ}C$ – $31.2^{\circ}C$, and completely at $234^{\circ}C$ – $357^{\circ}C$ (mainly $260^{\circ}C$ – $269^{\circ}C$) to liquid phase and (minor) to gaseous phase (Table 1; Figure 8). The fluid salinity is 3.52–11.61 (mainly 8.00–9.90) wt.% NaCleqv. (Figure 9), whilst the fluid pressure and density are 261–353 MPa and 0.73 – $0.94 g/cm^3$, respectively (Table 1). For type Ib ($L_{H_2O}+V_{CO_2}$) FIs, the ice-freezing and homogenization temperatures are $-5.4^{\circ}C$ – $5.6^{\circ}C$ and $234^{\circ}C$ – $276^{\circ}C$, respectively. The salinity is 8.03–8.41 wt.% NaCleqv., whilst the density is 0.83 – $0.97 g/cm^3$ (Table 1).

During the main-ore stages II and III, the smoky-gray quartz contains all four FI types (I to IV), but are dominated by type Ia. The FIs are mostly 5–10 μm in diameter and occur as isolation or in groups. Type Ia FIs are homogenized partially at $24.0^{\circ}C$ – $31.2^{\circ}C$, and completely at $229^{\circ}C$ – $299^{\circ}C$ (mostly $229^{\circ}C$ – $269^{\circ}C$) (Table 1; Figure 8). The FIs have 0.43–11.61 (mostly 4.00–7.90) wt.% NaCleqv. salinity (Figure 8), 217–321 MPa fluid pressure, and 0.73 – $0.94 g/cm^3$ density. Type IIa FIs have ice-freezing and homogenization temperatures of $-7.3^{\circ}C$ to $6.6^{\circ}C$ and $176^{\circ}C$ – $213^{\circ}C$, respectively. They have 3.39–10.86 wt.% NaCleqv. salinity and 0.83 – $0.97 g/cm^3$ density (Table 1).

Stage IV quartz has mainly type Ib FIs, with size of $2 \times 3 \mu m$. These FIs are clustered or randomly distributed, most of which are elliptical or irregular-shaped. The ice-freezing and total homogenization temperatures are $-5.6^{\circ}C$ – $6.8^{\circ}C$ and $175^{\circ}C$ – $264^{\circ}C$ ($175^{\circ}C$ – $209^{\circ}C$), respectively (Table 1; Figure 8). The FIs have 1.57–8.68 (6.00–9.90) wt.% NaCleqv. salinity, and 0.80 – $0.95 g/cm^3$ density (Figure 9; Table 1).

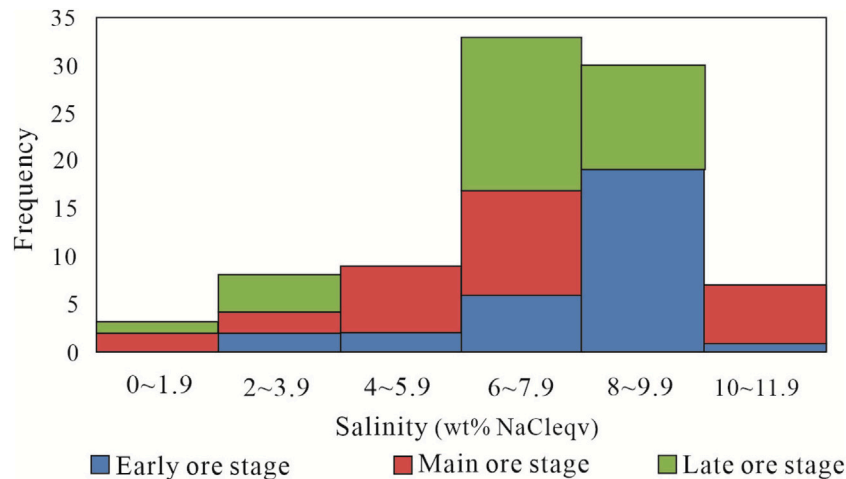


FIGURE 9
Salinity distribution histogram of fluid inclusions from the different metallogenic stages at Zhaoxian.

Fluid inclusion temperature of the various ore stages

The ore-fluid temperature and salinity decrease gradually from the early to late ore stage. Type Ia and Ib FIs with different phase ratios coexist in this stage, and they have similar homogenization temperature range (176°C–299°C) but different homogenization modes (homogenized to liquid and gas phase, respectively). The CO₂ content decreases markedly in the late ore stage (Table 1).

Stage I: The CO₂ liquid and gas phases of the FIs are homogenized to liquid. The partial (Th_{CO₂}) and total (Th_{tot}) homogenization temperatures are 28.5°C–31.2°C and 234°C–357°C, respectively.

Stage II and III: Both the CO₂ liquid and CO₂ gas phase in the FIs homogenized to liquid, with Th_{CO₂} = 24°C–31.2°C. The Th_{tot} of type Ia FIs is generally higher than that of type Ib FIs.

Stage IV: A small number of type II FIs are observed in quartz and calcite, but those in the calcite are not fit for microthermometric measurement. The ice-freezing and homogenization temperatures of type IIa FIs in quartz are -5.6°C–6.8°C and 175°C–264°C, respectively, with corresponding salinity of 1.57–8.68 wt.% NaCleqv.

Density

The following formula is used to calculate the density of type Ib and IIa FIs from Zhaoxian (Potter et al., 1977; Lu et al., 2004):

$$\rho = A + Bt + Ct^2$$

$$A = 0.993531 + 8.72147 \times 10^{-3} * S - 2.43975 \times 10^{-5} * S^2$$

$$B = 7.11652 \times 10^{-5} - 5.2208 \times 10^{-5} * S + 1.26656 \times 10^{-6} * S^2$$

$$C = -3.4997 \times 10^{-6} + 2.12124 \times 10^{-7} * S - 4.52318 \times 10^{-9} * S^2$$

where $t = Th_{tot}$ of the gas–liquid two-phase FIs (Th (°C)), S = salinity (wt.% NaCleqv.), and ρ = fluid density (g/cm³).

The following formula is used to calculate the density of ore-stage type I FIs from Zhaoxian (Potter et al., 1977; Lu et al., 2004):

$$\rho(I) = 0.4683 + 0.001441 * (3.35 - t) + 0.1318 * (3.35 - t) \frac{1}{3}$$

$$\rho = \varphi(CO_2) * \rho(I) + (1 - \varphi(CO_2)) * \rho(aq)$$

where $t = (Th_{CO_2})$ of the gas phase CO₂ (°C), $\varphi(CO_2)$ = volume percent of the CO₂ gas phase and liquid phase in the FIs (%), $\rho(I)$ = density of the CO₂ phase when homogenized to liquid

(g/cm³), $\rho(aq)$ = brine density (g/cm³), and ρ = ore fluid density (g/cm³).

The calculated density (0.73–0.97 g/cm³) is shown in Table 1. The density of type Ia FIs and type Ib and IIa FIs are 0.73–0.94 and 0.80–0.97 g/cm³, respectively, indicating that the fluid has low density.

Metallogenic depth estimation

The trapping pressure of our FI samples is 217–353 MPa (mainly 260–330 MPa). The metallogenic depth (H) is estimated to be 7.4–12.0 km with the equation of: $P = \rho g H$ ($\rho = 3$ g/cm³), where P = metallogenic pressure (Sheperd et al., 1985).

Laser Raman spectroscopic results

Representative type Ia, Ib and IIa were analyzed, and the resulting laser Raman spectra show characteristic CO₂ peaks (1,386 cm⁻¹, 1,285 cm⁻¹, 1,282 cm⁻¹) (Figure 10) and a slightly weaker CH₄ peak (2,912 cm⁻¹) (Figure 10). Laser Raman spectra also show that the early ore stage type Ia FIs has pure CO₂. Besides, the gas phase basically does not contain CH₄.

Trace element compositions of ore-stage granite

In this study, we have analyzed the sericite-pyrite-altered cataclastic granite ($n = 4$) (main-ore) and sericite-pyrite-altered cataclastic rocks ($n = 3$) (main-ore) from Zhaoxian, using the ME-MS81 method at the ALS Laboratory (Guangzhou) Co. Ltd. The analysis used an Elan9000 inductively coupled plasma mass spectrometer (ICP-MS) (United States), with better than 5% analytical accuracy (Xiao and Liao, 2016). Detailed sample preparation and analysis methods follow those of Zhang and Guo (2012). The data are given in Table 2. The ore-stage granites have the following geochemical characteristics: 1) low Nb/Ta ratios. The Nb/Ta is largely unaffected by fractionation. Tantalum and

TABLE 2 Trace element contents and ratios of syn-ore granite at Zhaoxian (trace element unit: ppm).

Sample number	ZX3	ZX9	ZX10	ZX21
Rb	3.3	3.2	1.5	0.7
Ba	10.1	68.1	30.6	15.9
Th	4.12	0.89	0.22	0.16
U	0.9	0.6	0.09	0.12
Ta	0.8	0.1	0.9	0.7
Nb	1.5	2.2	0.2	0.19
La	45.7	4.2	4.2	0.9
Ce	84.1	7.4	7.3	1.6
Sr	6.5	6.8	4.6	3.6
Nd	31.1	2.7	2.4	0.7
Zr	55	44	5	3
Hf	1.4	1.3	0.2	0.2
Sm	4.52	0.46	0.38	0.19
Y	3.8	2.8	1.5	1.6
Yb	0.27	0.24	0.13	0.09
Th/U	4.58	1.48	2.44	1.33
Rb/Sr	0.51	0.47	0.33	0.19
Rb/Ba	0.33	0.05	0.05	0.04
Rb/Nb	2.20	1.45	7.50	3.68
Zr/Hf	39.29	33.85	25.00	15.00
Nb/Ta	1.88	22.00	0.22	0.27

Unit of analysis: Aushi Analysis and Testing (Guangzhou) Co., Ltd.; Analysis method: ME-MS81 plasma mass spectrometry.

Nb is enriched and depleted in the crust, respectively, and thus the Nb/Ta ratio can indicate the degree of crustal involvement in magma formation (Green et al., 1995). The Nb/Ta ratio of our granite samples are 0.22 ± 1.88 (except for sample ZX9), which is significantly lower than the average Nb/Ta (11) of the post-Archean continental crust (Green et al., 1995).

During magmatic fractionation, Rb could replace K in K-feldspar, and Sr replaces Ca in plagioclase. Therefore, highly fractionated magma would have higher K-Rb and lower Ca-Sr. Our granite samples have high Rb/Sr (0.19–0.51, avg. 0.38), suggesting high degree of fractionation (Table 2). This is consistent with the low Zr/Hf and Th/U ratios of the granite samples (Zhang and Guo, 2012). The primitive mantle-normalized multielement plot for the granite samples shows that the granites are obviously enriched with large-ion lithophile elements (LILEs) such as Rb and Th, and depleted in Nb and Sr (Figure 11).

Discussion

Ore fluid properties and evolution

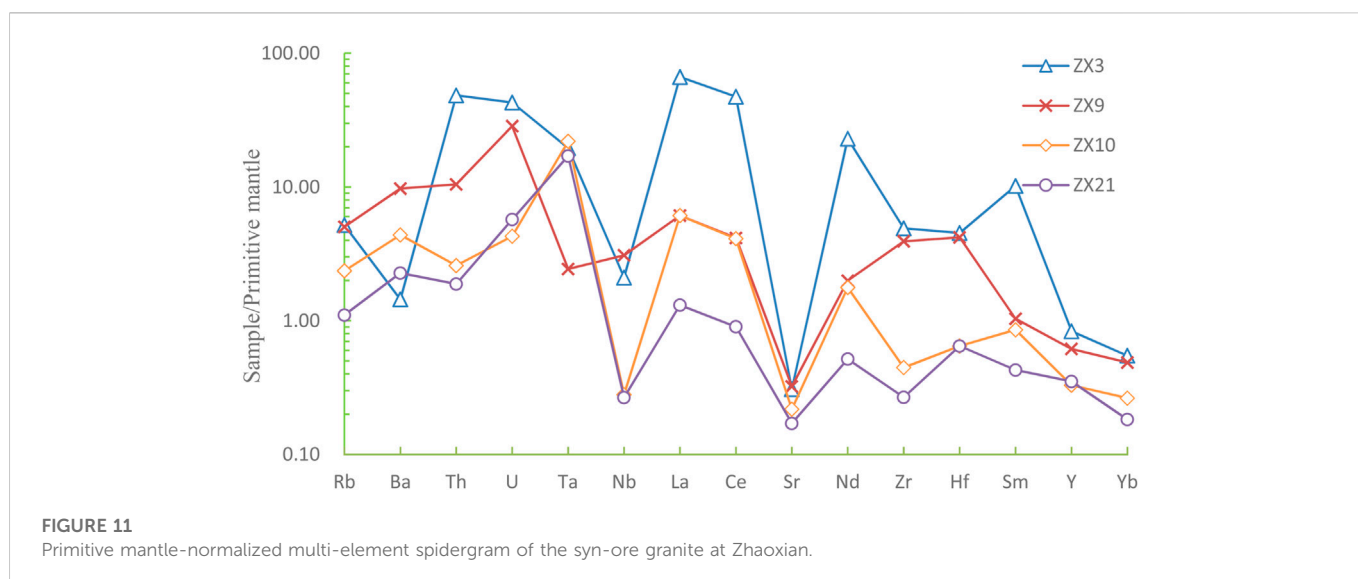
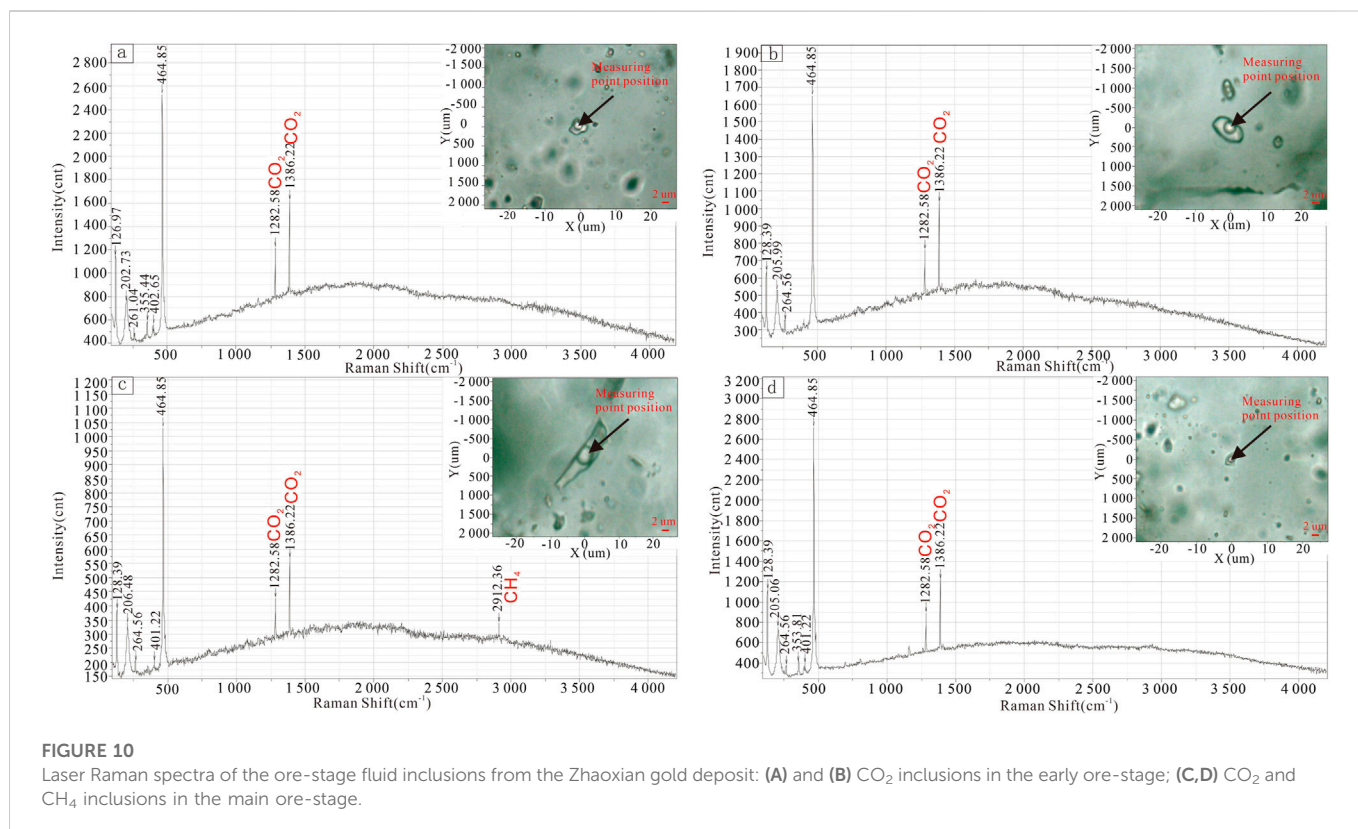
The FI petrographic, microthermometric and laser Raman spectroscopic data show that the ore fluids are of medium-low

salinity and belong to a CO₂-H₂O system, consistent with the published data from the shallow part of the Jiaojia gold deposit and most Jiaojia-type gold deposits in this area. The features are different from typical high-temperature and high-salinity magmatic ore-forming fluids, but resemble the ore-forming fluids of most orogenic-type gold deposits.

Our results show that the main ore stage fluids are hotter and are more CH₄-rich than those of the early ore stage. Some studies suggested that the early ore-forming fluids of Jiaojia-type gold deposits are CO₂-rich and CH₄-poor, while the main ore stage fluids contain more CH₄ (Fan et al., 2005; Wen et al., 2016). There are two possible sources of CH₄: 1) re-equilibrium by the infiltration of H₂ into the FIs (Hall and Bodnar, 1990; Ridley and Hagemann, 1999); 2) the H₂O-NaCl-CO₂ fluids produced a small amount of CH₄ with the decreasing temperature and oxygen fugacity from the early to main ore stage.

Because the fluid immiscibility would cause substantial CO₂ loss, the temperature drop would lead to a decrease in the SiO₂ solubility, forming the late-stage quartz-calcite veins (Shu et al., 2022). The low salinity in type II FIs suggests that the late-stage fluids are of low-salinity and CO₂-poor.

In the early ore stage, the FIs are dominantly CO₂-bearing three-phase, and thus the ore-forming fluid is CO₂-rich and of high



temperature. Metal complexes are stable in this weakly acidic hydrothermal fluid, and thus it could dissolve and carry gold and other ore-forming elements (Yang, 1986; Liu and Shen, 1999; Phillips et al., 2004; Hou et al., 2007; Lu, 2011; Mao et al., 2013).

The homogenization temperature of type Ia FIs is higher than those of type Ib FIs, and the salinity and density of type Ib FIs are lower than those of type Ia FIs. This may be caused by fluid immiscibility (Huang, 2021). During fluid immiscibility, the homogeneous temperature and pressure of inclusions are similar

and can represent the fluid trapping temperature and pressure. (Huang, 2021). Therefore, the homogenization temperature of type Ia FIs can represent the capture temperature of immiscible inclusions, i.e., the ore-forming temperature is 234°C–357°C. The formation of many CO₂-bearing three-phase inclusions in quartz indicates that the fluid is CO₂-rich or carbonic. The presence of CO₂ can increase the solubility of chlorine and water in magmatic fluids and facilitate metal migration (Rui et al., 2003; Chen et al., 2006).

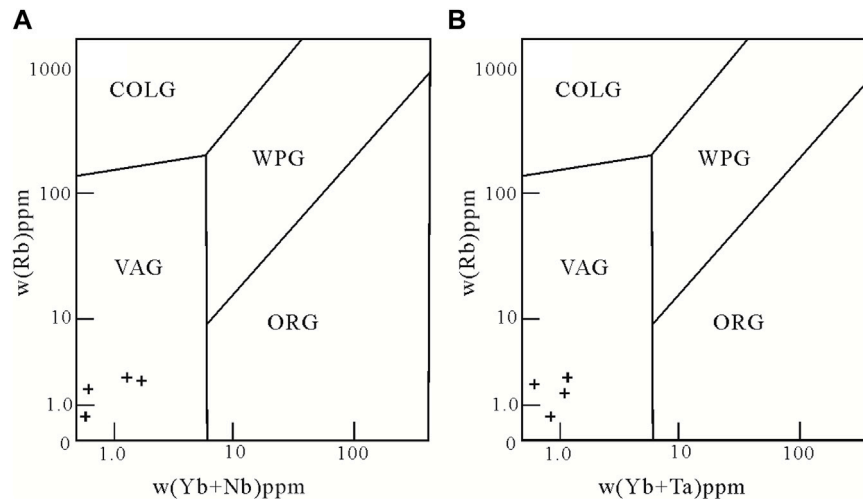


FIGURE 12

Trace element tectonic discrimination diagrams for granites (modified from Pearce, 1984): Yb+Nb-Rb (A); Yb+Ta-Rb (B) tectonic discrimination diagrams; VAG-Volcanic arc granite; ORG-Ocean ridge granite; WPG-Within-plate granite; COLG-Collision granite.

Source of ore-forming materials

According to previous studies, the ore-forming materials in northwestern Jiaodong gold province were mainly derived from the Jiaodong metamorphic rocks (Deng et al., 2004; Li et al., 2007; Guo et al., 2008; Liang et al., 2015), yet the average gold content of the latter (2.47 ppb) is lower than that of the crust average (4 ppb) (Li and Ni, 1990). The average Au content of the Neoproterozoic Jiaodong Group metagabbro in the Jiaojia fault hanging-wall at Zhaoxian is low (1.16 ppb) (Yang et al., 1991), and could unlikely represent a main gold source. The Au content of Linglong granite (19 ppb) and Guojialing granite (49 ppb) in the Jiaodong district area are higher (Lu et al., 1999; Xu et al., 2022), and both being interpreted to have a crust-mantle mixed magma source. An upper mantle source of Au has also been suggested for the Jiaodong gold deposits (Gui, 2014).

In the geochemical tectonic discrimination plots for granites (Figure 12), our granite samples all fall inside the volcanic arc granite field, reflecting that they were formed in an arc setting (Pearce et al., 1984).

Thus, the granites at Zhaoxian may have emplaced in an arc environment, with its formation related to mantle-derived magma underplating. The mantle source may have provided both the heat to partially melt the crust and mix with the crustal magma (Zhang and Guo, 2012). Our geochemical data on the Zhaoxian granite show that the granite is highly fractionated with dominantly continental crustal source. Therefore, we infer that the gold ore-forming materials were mainly derived from the upper mantle. During the upwelling of mantle materials, gold may have ascended with the magma and formed gold deposits.

Source of ore-forming fluid and the gold metallogeny

Based on the close spatial relationship of the Jiaodong gold deposits with the Jiaodong Group metamorphic rocks, Linglong

granite, and Guojialing granodiorite. Many works in the 1980s and 1990s proposed that the ore-forming fluids were magmatic-hydrothermal sourced with meteoric water input (Wang and Li, 1985; Zhang et al., 1994; Wang et al., 1995; Zhang et al., 1995; Lin and Yin, 1998). In recent years, some works have invoked mantle-derived input for the ore fluids in the Jiaodong gold province, based on mineral isotope and FI studies (Sun and Shi, 1995; Mao et al., 2002; Zhang et al., 2002; Liu et al., 2003; Fan et al., 2005).

Published He and Ar isotope data of FIs in pyrite from the Dengezhuang and Jiaojia gold deposits indicated that the ore-forming fluids have high $3\text{He}/^4\text{He}$ and $40\text{Ar}/^{36}\text{Ar}$ values, resembling mantle-derived fluids (Zhang et al., 2002). By studying the carbonate minerals from the Rushan and Jiaojia gold deposits, Liu et al. (2003) concluded that the Sr-Nd isotopic compositions are similar to those of the mantle source rocks.

The northwest Jiaodong region has experienced a complex tectonic evolution. In the Late Jurassic, the regional tectonics was influenced by the Paleo-Pacific subduction beneath Eastern China. Since the Early Cretaceous, regional tectonics had evolved from intracontinental compressional orogeny and crustal thickening to intracontinental rifting and lithospheric thinning. The Paleo-Pacific subduction had also led to sinistral shearing of the transcrustal Tanlu (Yishu) fault and its associated NE-NNE-trending structures. The transtension may have provided open space for the ascent of deep magmatic fluid (and thus gold mineralization) and mafic dyke intrusion (Goldfarb and Groves, 2015; Guo, 2016; Dou et al., 2021). During the upwelling of mantle material, gold may have ascended with the magma, and deposited at the open-space formed by the transtensional faults.

Conclusion

1) The gold ore-forming fluid at Zhaoxian belongs to a medium-to low-salinity $\text{H}_2\text{O}-\text{NaCl}-\text{CO}_2 \pm \text{CH}_4$ system. The main types of

FIs (FIs) in quartz are CO₂-H₂O (type I) and H₂O aqueous (type II). Early- and main-stage mineralization involves mainly type II and type I, respectively. The phase proportion changes substantially, and the CH₄ content increases markedly with ore-fluid evolution. The syn-ore FIs have medium-low homogenization temperature (234°C–357°C) and low salinity (3.52–11.61 wt.%NaCleqv). The ore-fluid pressure and density are estimated to be ca. 217–353 MPa (medium-low pressure) and 0.73–0.97 g/cm³ (low density), respectively, yielding medium-large ore-forming depth of 7.4–12.0 km.

- 2) Trace element characteristics of ore-stage granites at Zhaoxian inferred that the gold ore-forming materials at Zhaoxian were mainly derived from deep source, possibly associated with asthenospheric upwelling.
- 3) In the Mesozoic, the NW-dipping subduction of Paleo-Pacific plate under Eurasia may have resulted in the left-lateral shear of the Tanlu fault zone, and the Jiaodong region had undergone intense tectonic deformation and magmatism. During the Mesozoic regional tectonic transition, the Tanlu fault and its secondary structures may have opened by the transtension and provided channels for the ascending deep magmatic-sourced fluids. These fluids may have mixed with the metamorphic water and meteoric water circulating in the middle-upper crust, and eventually led to the gold mineralization (Song et al., 2018).

Data availability statement

The raw data supporting the conclusions of this article will be made available by the authors, without undue reservation.

References

- Brown, P. E., Hageman, S. G., and Vanko, D. A. (1995). MacFlinCor and its application to fluids in Archean lode-gold deposits. *Geochimica Cosmochimica Acta* 59 (19), 3943–3952. doi:10.1016/0016-7037(95)00254-w
- Cao, X. H., Meng, Q. W., and Cao, Y. Y. (2016). Application of comprehensive geophysical method to gold prospecting in the southern section of Jiaojia fault. *Shandong Land Resour.* 32 (8), 66–73.
- Chen, G. Y., Shao, W., and Sun, D. S. (1989). *Genetic mineralogy and prospecting of Jiaodong gold deposit*. Chongqing, China: Chongqing Publishing House.
- Chen, Y. J. (2006). Orogenic deposits, metallogenic model and prospecting potential. *Geol. China* 33 (6), 1181–1196.
- Deng, J., Liu, X., Wang, Q., and Pan, R. (2015). Origin of the Jiaodong-type Xinli gold deposit, Jiaodong Peninsula, China: Constraints from fluid inclusion and C–D–O–S–Sr isotope compositions. *Ore Geol. Rev.* 65, 674–686. doi:10.1016/j.oregeorev.2014.04.018
- Deng, J., Wang, Q. F., and Yang, L. Q. (2004). The geological background of mineralization in the gold concentration area of northwest Jiaotang. *Geosci. Front.* 4, 527–533.
- Dou, Y. X., Mao, G. Z., Meng, L. Q., Liu, X., An, P., and Cao, M. (2021). Fluid and ore-material source of the Xiajiaxiaohu gold deposit in central Yishu fault zone in Shandong, Eastern China. *Arabian J. Geosciences* 14, 26. doi:10.1007/s12517-020-06288-5
- Fan, H. R., Hu, F. F., and Yang, J. H. (2005). Fluid evolution and large-scale gold mineralization during Mesozoic tectonic regime transition in Jiaodong. *Acta Petrol. Sin.* 21 (5), 1317–1328.
- Goldfarb, R. J., and Groves, D. I. (2015). Orogenic gold: Common or evolving fluid and metal sources through time. *Lithos* 233, 2–26. doi:10.1016/j.lithos.2015.07.011
- Green, T. H., McDonough, W. F., and Arndt, N. T. (1995). Significance of Nb/Ta as an indicator of geochemical processes in the crust-mantle system. *Chem. Geol.* 120 (3–4), 347–359. doi:10.1016/0009-2541(94)00145-x
- Gui, F. (2014). *Discussion on mineralization and enrichment regularity and genesis of Sanshandao gold deposit in Laizhou*. Shandong, China: Jilin University.
- Guo, B., Liu, Z. C., and Li, W. (2008). Metallogenic geological characteristics and prospecting prediction of Sanshandao gold deposit. *Min. Eng.* 4, 14–16.
- Guo, L. N. (2016). *Metallogenic mechanism of Jiaodong type gold deposit*. Beijing, China: Doctoral thesis of China University of Geosciences.
- Hall, D. L., and Bodnar, R. J. (1990). Methane in fluid inclusions from granulites: A product of hydrogen diffusion. *Pergamon* 54 (3), 641–651. doi:10.1016/0016-7037(90)90360-w
- He, C. Y., Guo, G. Q., and Liu, C. W. (2015). Study on ore-controlling structural belt and analysis of metallogenic prospect in the covered area of southern Jiaojia fault zone. *Shandong Land Resour.* 7, 19–24.
- Hou, M. L., Jiang, S. Y., and Shen, K. (2007). Geochemistry of fluid inclusions and hydrogen and oxygen isotopes in Penglai gold mining area, Jiaodong. *Acta Petrol.* 9, 2241–2256.
- Hu, Z. L., Jiang, X. H., and Liang, G. Z. (2021). Vertical variation characteristics of ore-forming fluid in Jiaojia gold deposit and its enlightenment to Jiaodong gold metallogenic process. *Mineral Rock Geochem. Bull.* 40 (6), 1345–1356.
- Huang, X., Zhang, T., Zhao, F., Feng, G., Liu, J., Yang, G., et al. (2021). Effects of cryopreservation on acrosin activity and DNA damage of Russian sturgeon (*Acipenser gueldenstaedtii*) semen. *Geol. Northwest China* 54 (4), 129–136.
- Li, G. H., Ding, Z. J., and Song, M. C. (2017). A new type of gold deposit in Jiaodong-Liaoshang pyrite carbonate vein type gold deposit. *Acta Geol. Sin.* 38 (3), 423–429.
- Li, H. M., Shen, Y. C., and Mao, J. W. (2003). Rare Earth element characteristics of quartz, pyrite and their inclusions-taking Jiaojia type gold deposit in Jiaodong as an example. *Acta Petrol.* 19 (2), 267–274.
- Li, S. X., Liu, C. C., and An, Y. H. (2007). *Geology of Jiaodong gold deposit*. Beijing, China: Geological Publishing House.
- Li, T., and Ni, S. B. (1990). *Abundance of chemical elements in the earth and crust*. Beijing, China: Geological Publishing House.

Author contributions

All authors listed have made a substantial, direct, and intellectual contribution to the work and approved it for publication.

Funding

The work was funded by the National Natural Science Foundation of China (42172087, 41772125, 41572063), Shandong Provincial Engineering Laboratory of Big Data Application and Development for Deep Gold Exploration (SDK202208), and the Key Laboratory of Gold Ore Formation Process and Resource Utilization (Ministry of Land and Resources) (2013003). We would like to thank the Analysis and Testing Research Center (Beijing Geological Research, Institute of Nuclear Industry) and the ALS Laboratory (Guangzhou) Co., Ltd. for the analytical work.

Conflict of interest

The authors declare that the research was conducted in the absence of any commercial or financial relationships that could be construed as a potential conflict of interest.

Publisher's note

All claims expressed in this article are solely those of the authors and do not necessarily represent those of their affiliated organizations, or those of the publisher, the editors and the reviewers. Any product that may be evaluated in this article, or claim that may be made by its manufacturer, is not guaranteed or endorsed by the publisher.

- Li, X. M. (1988). Study and application of oxygen, hydrogen and carbon stable isotopes in Sanshandao gold deposit, Shandong. *Geol. Prospect.* 3, 62–71.
- Li, Y. D. (2016). Analysis of geological background and distribution characteristics of gold deposits in Jiaodong area. *World Nonferrous Met* 458, (14), 92–93.
- Liang, Y. Y., Liu, X. F., and Liu, L. L. (2015). Micro-area geochemical characteristics of gold minerals in altered rock type gold deposits in Jiaodong. *Acta Petrol. Sin.* 31 (11), 3441–3454.
- Lin, W. W., and Yin, X. L. (1998). Geological characteristics of isotopes of ore-forming fluids in Jiaodong gold deposit. *J. Rock Mineralogy* 3, 58–68.
- Liu, B., and Shen, K. (1999). *Thermodynamics of fluid inclusions*. Beijing, China: Geological Publishing House.
- Liu, J. M., Zhang, H. F., and Sun, J. G. (2003). Carbon-oxygen and strontium-neodymium isotope geochemistry of mantle-derived magmatic rocks in Shandong. *Chin. Sci. Ser. D* 10, 921–930.
- Lu, H. Z., Fan, H. R., and Ni, P. (2004). *Fluid inclusions*. Beijing, China: Science Press.
- Lu, H. Z. (2011). Fluid immiscibility and fluid inclusion. *Acta Petrol. Sin.* 27 (5), 1253–1261.
- Lu, H. Z., Guy, A., Li, Y. S., and Wei, J. X. (1999a). Relationship between deformation types and gold deposits in Linglong-Jiaojia area, Shandong Province. *Acta Geol. Sin.* 2, 174–188.
- Lu, H. Z., and Fang, G. B. (1999b). Characteristics of ore-forming fluid in Linglong gold deposit, Shandong. *Geochemistry* 28 (05), 421–437.
- Ma, W., Fan, H., Liu, X., Pirajno, F., Hu, F. F., and Yang, K. F., (2017). Geochronological framework of the Xiadian gold deposit in the Jiaodong province, China: Implications for the timing of gold mineralization. *Ore Geol. Rev.* 86, 196–211. doi:10.1016/j.oregeorev.2017.02.016
- Mao, G. Z., Hua, R. M., Long, G. M., and Lu, H. J. (2013). Rb-Sr dating of pyrite and quartz fluid inclusions and origin of ore-forming materials of the jinshan gold deposit, northeast Jiangxi province, south China. *Acta Geol. Sin.* 87 (6), 1658–1667. doi:10.1111/1755-6724.12166
- Mao, J. W., He, Y., and Ding, T. P. (2002). Carbon, oxygen and hydrogen isotope evidence that mantle fluid is involved in the metallogenic process during the formation of Jiaodong gold deposit. *Depos. Geol.* 2, 121–128.
- Pearce, J. A., Harris, N. B. W., and Tindle, A. G. (1984). Trace element discrimination diagrams for the tectonic interpretation of granitic rocks. *J. petrology* 25 (4), 956–983. doi:10.1093/ptrology/25.4.956
- Phillips, G. N., and Evans, K. A. (2004). Role of CO₂ in the formation of gold deposits. *Nature* 429 (6994), 860–863. doi:10.1038/nature02644
- Potter, R. W. (1977). Pressure corrections for fluid inclusion homogenization temperatures based on the volumetric properties of the system NaCl-H₂O. *USGSJ Res.* 5 (05), 603–607.
- Qiu, Y. S., Yang, G. H., and Wang, K. H. (1988). *Regional metallogenic conditions of gold deposits in Zhaoyuan-Yexian area, Shandong*. Shenyang, China: Liaoning Science and Technology Press.
- Ridley, J., and Hagemann, S. G. (1999). Interpretation of post-entrapment fluid-inclusion re-equilibration at the three mile hill, marvel loch and griffins find high-temperature lode-gold deposits, yilgarn Craton, western Australia. *Chem. Geol.* 154 (1), 257–278. doi:10.1016/S0009-2541(98)00135-1
- Rui, Z. Y., Li, Y. Q., and Wang, L. S. (2003). The metallogenic conditions of metal deposits are discussed from the study of fluid inclusions. *Geol. Depos.* 1, 13–23.
- Shepherd, T. J., Rankin, A. H., and Alderton, D. M. (1985). *A practical guide to fluid inclusion studies*. London, UK: Chapman & Hall.
- Shu, L., Shen, K., and Yu, X. F. (2022). Characteristics of ore-forming fluid inclusions in the deep part of Jiaojia fault zone, northwest Jiaozhou. *Geol. Bull.* 41 (6), 1068–1080.
- Song, G. Z., Li, S., and Yan, C. M. (2018). Geological characteristics and prospecting direction of main orebody I in Jiaojia Gold Orefield. *Geol. Explor.* 54 (2), 219–229.
- Song, M. C., Cui, S. X., and Zhou, M. L. (2010b). Deep super-large gold deposit in Jiaojia mining area, Shandong Province and its enlightenment to “Jiaojia type” gold deposit. *Acta Geol. Sin.* 84 (9), 1349–1358.
- Song, M. C., Lin, S. Y., and Yang, L. Q. (2020). Metallogenic model of Jiaodong gold deposit. *Depos. Geol.* 39 (2), 215–236.
- Song, M. C., Wang, H. J., and Cui, S. X. (2010a). Relationship between deep and shallow gold deposits in the main metallogenic belt of northwest Jiaotang. *Geol.* 29 (S1), 989–990.
- Sterner, S. M., and Bodnar, R. J. (1991). Synthetic fluid inclusions: X. Experimental determination of P-V-T-X properties in the CO₂-H₂O system to 6kb and 200 °C. *Amer. J. Sci.* 29 (1), 1–54. doi:10.2475/ajs.291.1.1
- Sun, F. Y., and Shi, J. L. (1995). On the relationship between mantle-derived C-H-O fluids and some geological processes in the continental plate. *Geosci. Front.* 2, 167–174.
- Sun, T., Wang, C. T., and Wang, H. Z. (2018). Study on the strike and ore-controlling characteristics of the eastern segment of the Hexi fault in the Jiaojia fault zone. *Shandong Land Resour.* 34 (2), 8–12.
- Tan, J., Wei, J., Audétat, A., and Pettko, T. (2012). Source of metals in the Guocheng gold deposit, Jiaodong Peninsula, North China Craton: Link to early Cretaceous mafic magmatism originating from Paleoproterozoic metasomatized lithospheric mantle. *Ore Geol. Rev.* 48, 70–87. doi:10.1016/j.oregeorev.2012.02.008
- Tan, J., Wei, J., He, H., Su, F., Li, Y., and Fu, L. (2018). Noble gases in pyrites from the Guocheng-Liaoshang gold belt in the Jiaodong province: Evidence for a mantle source of gold. *Chem. Geol.* 480, 105–115. doi:10.1016/j.chemgeo.2017.09.027
- Tang, J., Zheng, Y. F., Wu, Y. B., Gong, B., and Liu, X. (2007). Geochronology and geochemistry of metamorphic rocks in the Jiaobei terrane: Constraints on its tectonic affinity in the Sulu orogen. *Precambrian Res.* 152 (1/2), 48–82. doi:10.1016/j.precamres.2006.09.001
- Tang, J., Zheng, Y. F., Wu, Y. B., Gong, B., Zha, X., and Liu, X. (2008). Zircon U–Pb age and geochemical constraints on the tectonic affinity of the Jiaodong terrane in the Sulu orogen, China. *Precambrian Res.* 161 (3/4), 389–418. doi:10.1016/j.precamres.2007.09.008
- Touret, J., and Bottinga, Y. (1979). Equation of state of CO₂: Application to carbonic inclusions. *Bull. Mineral.* 10 (2), 577–583. doi:10.3406/bulmi.1979.7306
- Wang, B. C., and Li, F. T. (1985). Petrological and mineralogical characteristics of Linglong granite. *Shandong Geol.* 115 (1), 1–25.
- Wang, B. C., Xu, J. F., and Zheng, W. S. (1995). Argon, hydrogen and oxygen stable isotope geochemistry and deposit Genesis of some gold deposits in Jiaodong, Shandong. *Precious Met. Geol.* 1, 24–35.
- Wang, L., Pan, Z. C., and Sun, L. W. (2014). Fluid inclusions in the Xincheng gold deposit, Laizhou, Shandong. *J. Jilin Univ. (Geoscience Ed.)* 44, 1166–1176.
- Wang, Y. P., Zhang, W., Li, X. Z., Liu, H. D., Zhu, P. G., and Wang, L. G. (2022). New progress in deep prospecting and research of zhaoxian gold deposit in Jiaodong northwest region. *Shandong Land Resour.* 38 (9), 1–7.
- Wei, Q., Fan, H. R., and Lan, T. G. (2015). Genesis of the sizhuang gold deposit in Jiaodong: Evidence of fluid inclusions and quartz solubility. *Acta Lithol. Sin.* 31, 1016–1029.
- Wen, B., Fan, H., Hu, F., Liu, X., Yang, K. F., Sun, Z. F., et al. (2016). Fluid evolution and ore Genesis of the giant Sanshandao gold deposit, Jiaodong gold province, China: Constraints from geology, fluid inclusions and H–O–S–He–Ar isotopic compositions. *J. Geochem. Explor.* 171, 96–112. doi:10.1016/j.jexplo.2016.01.007
- Xiao, D., Liao, Q. N., and Wang, L. Y. (2016). Petrogenesis and tectonic significance of early Silurian granites in eastern Junggar. *J. geomechanics* 22 (4), 1049–1061.
- Xu, W., Fan, H., Yang, K., Hu, F. F., Cai, Y. C., and Wen, B. J. (2016). Exhaustive gold mineralizing processes of the Sanshandao gold deposit, Jiaodong Peninsula, eastern China: Displayed by hydrothermal alteration modeling. *J. Asian Earth Sci.* 129, 152–169. doi:10.1016/j.jseas.2016.08.008
- Xu, Y. W., Mao, G. Z., Liu, X. T., An, P., Wang, Y., and Cao, M. (2022). Genesis of the zhaoxian gold deposit, Jiaodong peninsula, China: Insights from *in-situ* pyrite geochemistry and S-He-Ar isotopes, and zircon U-Pb geochronology. *Front. Earth Sci.* 10, 886975. doi:10.3389/feart.2022.886975
- Yan, Y., Zhang, N., Li, S., and Li, Y. (2014). Mineral chemistry and isotope geochemistry of pyrite from the Heilangou gold deposit, Jiaodong Peninsula, Eastern China. *Geosci. Front.* 5 (2), 205–213. doi:10.1016/j.gsf.2013.05.003
- Yang, K. F., Fan, H. R., Santosh, M., Hu, F. F., Wilde, S. A., Lan, T. G., et al. (2012). Reactivation of the Archean lower crust: Implications for zircon geochronology, elemental and Sr-Nd-Hf isotopic geochemistry of late Mesozoic granitoids from northwestern Jiaodong Terrane, the North China Craton. *Lithos* 146/147, 112–127. doi:10.1016/j.lithos.2012.04.035
- Yang, L., Deng, J., Guo, L., Wang, Z. L., Li, X. Z., and Li, J. L. (2016a). Origin and evolution of ore fluid, and gold-deposition processes at the giant Taishang gold deposit, Jiaodong Peninsula, eastern China. *Ore Geol. Rev.* 72, 585–602. doi:10.1016/j.oregeorev.2015.08.021
- Yang, L., Deng, J., Wang, Z., Zhang, L., Goldfarb, R. J., and Yuan, W. M. (2016b). Thermochronologic constraints on evolution of the Linglong metamorphic core complex and implications for gold mineralization: A case study from the xiadian gold deposit, Jiaodong peninsula, eastern China. *Ore Geol. Rev.* 72, 165–178. doi:10.1016/j.oregeorev.2015.07.006
- Yang, L., Guo, L., Wang, Z., Zhao, R. X., Song, M. C., and Zheng, X. L. (2017). Timing and mechanism of gold mineralization at the Wang’ershan gold deposit, Jiaodong Peninsula, eastern China. *Ore Geol. Rev.* 88, 491–510. doi:10.1016/j.oregeorev.2016.06.027
- Yang, L. Q., Deng, J., and Ge, L. S. (2006). A review of the study on the metallogenic age and Genesis of Jiaodong gold deposits. *Adv. Nat. Sci.* 16 (07), 797–802.
- Yang, L. Q., Deng, J., and Wang, Z. L. (2014). Mesozoic gold metallogenic system in Jiaodong. *Acta Petrol. Sin.* 30 (9), 2447–2467.
- Yang, S. W. (1986). On the stratabound properties of Jiaodong Group strata, gold source beds and gold deposits in the northwest of Jiaodong Peninsula. *Ser. Geol. Prospect.* 1 (2), 1–12.
- Yang, Z. F., Xu, J. K., and Zhao, L. S. (1991). Study on hydrogen and oxygen isotopes of quartz inclusions and geochemistry of ore-forming fluid components in two genetic series gold deposits in Jiaodong. *J. Mineralogy* 11 (04), 363–369.
- Zhai, M., and Santosh, M. (2013). Metallogeny of the North China Craton: Link with secular changes in the evolving earth. *Gondwana Res.* 24 (1), 275–297. doi:10.1016/j.gr.2013.02.007

- Zhang, C. H., Liu, Y., and Liu, X. D. (2014). Sulfur isotope geochemistry of Xincheng gold deposit, northwest Jiaotong. *Acta Petrol. Sin.* 30 (9), 2495–2506.
- Zhang, L. C., Shen, Y. C., and Li, H. M. (2002). He and Ar isotopic compositions of fluid inclusions and source of ore-forming fluids in gold deposits in Jiaodong area. *Acta Petrol. Sin.* 18 (04), 559–565.
- Zhang, L. G., Chen, Z. S., and Liu, J. X. (1995). Study on water-rock exchange-hydrogen and oxygen isotope composition of altered rocks in Jiaojia type gold deposits. *Depos. Geol.* 14 (03), 261–272.
- Zhang, L. G., Chen, Z. S., and Liu, J. X. (1994). Study on water-rock exchange-hydrogen and oxygen isotope composition of ore-forming fluid in Jiaojia type gold deposit. *Depos. Geol.* 13 (3), 193–200.
- Zhang, L., Yang, L., Wang, Y., Weinberg, R. F., An, P., and Chen, B. Y. (2017). Thermochronologic constrains on the processes of formation and exhumation of the Xinli orogenic gold deposit, Jiaodong Peninsula, eastern China. *Ore Geol. Rev.* 81, 140–153. doi:10.1016/j.oregeorev.2016.09.026
- Zhang, W. S., and Guo, J. (2012). Geological and geochemical characteristics and Genesis of granites in the Naotan copper polymetallic mining area, Laos. *Chin. J. Nonferrous Metals* 22 (3), 686–693.
- Zhao, Y., Huang, Y. H., and Liang, K. (2015). Characteristics of rare Earth and trace elements of gold-bearing pyrite in Zhenyuan gold deposit, Sanjiang area, southwest China. *Acta Petrol. Sin.* 31 (11), 3297–3308.
- Zhou, T., and Guxian, L. (2000). Tectonics, granitoids and mesozoic gold deposits in East Shandong, China. *Ore Geol. Rev.* 16 (1-2), 71–90. doi:10.1016/s0169-1368(99)00023-2
- Zhu, D. C., Zhang, W., and Wang, Y. P. (2018). Orebody characteristics and prospecting prospect of Zhaoxian gold mining area in Laizhou City, Shandong Province. *Shandong Land Resour.* 34 (9), 14–19.